Journal of Computational Physics 227 (2008) 8992–9004

Contents lists available at ScienceDirect

Journal of Computational Physics

journal homepage: www.elsevier.com/locate/jcp

Split local absorbing conditions for one-dimensional nonlinear Klein-Gordon equation on unbounded domain

Houde Han *, Zhiwen Zhang

Department of Mathematical Sciences, Tsinghua University, Beijing 100084, PR China

ARTICLE INFO

Article history:
Received 24 January 2008
Received in revised form 26 May 2008
Accepted 9 July 2008
Available online 18 July 2008

Keywords:
Nonlinear Klein-Gordon equation (NKLGE)
Operator splitting method
Split local absorbing boundary
Soliton
Unbounded domain

ABSTRACT

The numerical solution of the one-dimensional nonlinear Klein-Gordon equation on an unbounded domain is studied in this paper. Split local absorbing boundary (SLAB) conditions are obtained by the operator splitting method, then the original problem is reduced to an initial boundary value problem on a bounded computational domain, which can be solved by the finite difference method. Several numerical examples are provided to show the advantages and effectiveness of the given method, and some interesting collision behaviors are also observed.

1. Introduction

The nonlinear Klein-Gordon equation (NKLGE) appears in various application areas, such as differential geometry and relativistic field theory, and it also appears in a number of other physical applications, including the propagation of fluxons in the Josephson junctions, the motion of rigid pendula attached a stretched wire, and dislocations in crystals [1,2].

The initial value problem of the one-dimensional nonlinear Klein-Gordon equation is given by the following problem:

$$\frac{\partial^2 u}{\partial t^2} - \frac{\partial^2 u}{\partial x^2} + f(u) = 0 \quad \forall x \in \mathbb{R}^1, t > 0, \tag{1.1}$$

$$u|_{t=0} = \varphi_0(x), u_t|_{t=0} = \varphi_1(x) \quad \forall x \in \mathbb{R}^1, \tag{1.2}$$

where $u = u(x,t)$ represents the wave displacement at position x and time t, $\varphi_0(x)$, $\varphi_1(x)$ are initial values, and $f(u)$ is the nonlinear force. In the well known sine-Gordon equation[19–21], the nonlinear force is given by

$$f(u) = \sin u. \tag{1.3}$$

In the physical applications, the nonlinear force $f(u)$ also has other forms [20–25]:

$$f(u) = u^3 - u, \tag{1.4}$$

$$f(u) = \sin u + \sin 2u, \tag{1.5}$$

$$f(u) = \sinh u + \sinh 2u. \tag{1.6}$$

* Corresponding author. Tel.: +86 10 6278 8979.
E-mail addresses: hhan@math.tsinghua.edu.cn (H. Han), zhangzhiwen02@mails.tsinghua.edu.cn (Z. Zhang).

0021-9991/$ - see front matter © 2008 Published by Elsevier Inc.
doi:10.1016/j.jcp.2008.07.006

Eq. (1.1) is called the ϕ^4 equation, the double sine-Gordon (DSG) equation and the double sinh-Gordon (DSHG) equation, provided $f(u)$ is given by (1.4)–(1.6), respectively. The above nonlinear Klein-Gordon equations are Hamiltonian PDEs, and for a wide class of force $f(u)$, it has the conserved Hamiltonian quantity (or energy) [21]

$$H = \int \left(\frac{1}{2}u_t^2 + \frac{1}{2}u_x^2 + G(u)\right)\mathrm{d}x,$$

where $G'(u) = f(u)$.

The essential difficulty of the numerical solution for the problem (1.1) and (1.2) involves two parts, the nonlinearity and the unboundedness of the physical domain. For the bounded domain case, there are a lot of studies on the numerical solution of the NLKGE with Dirichlet or periodic boundary condition. For example, Li and Vu-Quoc [3] studied the finite difference invariant structure of a class of algorithms for the nonlinear Klein-Gorodn equation and derived algorithms that preserve energy or linear momentum. Jiminez [4], Jiminez and Vazquez [5] discussed four second-order finite difference schemes for approximating the nonlinear Klein-Gordon equation with periodic boundary condition. They also observed the undesirable characteristics in some of the numerical schemes, in particular a loss of spatial symmetry and the onset of instability for large value of a parameter in the initial condition of the equation. Guo et al. [6] used the spectral and pseudo-spectral methods to solving the nonlinear Klein-Gordon equation. Guo et al. [7] also investigated the Numerical solution of the sine-Gordon equation with periodic boundary condition. In this paper, we will consider the NLKGE on an unbounded domain.

The artificial boundary condition (ABC) method is a powerful approach to reduce the problems on the unbounded domain to a bounded computational domain. In general, the artificial boundary conditions can be classified into implicit boundary conditions and explicit boundary conditions including global, also called nonlocal ABC, local ABC and discrete ABC [11]. For the last 30 years, many mathematicians have made great contributions on this subject, see [8–15], which makes the artificial boundary condition method for the linear partial differential equations on the unbounded domain become a well-developed method. In recent few years, there have been some new progress on the artificial boundary condition method for nonlinear partial differential equations on unbounded domain. Han et al. [16] and Xu et al. [17] use the Cole–Hopf transformation to get the exact ABCs for the viscous Burger's equation and the deterministic KPZ equation, Zheng [18,19] use the inverse scattering approach to get the exact ABCs for the one-dimensional cubic nonlinear Schrödinger equation and the sine-Gordon equation. Xu et al. [31,32] also utilize an operator splitting method to design split local absorbing boundary (SLAB) conditions for the one- and two-dimensional nonlinear Schrödinger equations. The local absorbing boundary conditions were imposed on the split linear subproblem and yielded a full scheme by coupling the discretizations for the interior equation and boundary subproblems.

In this paper, we use the operator splitting method to find the split local absorbing boundary (SLAB) conditions for the nonlinear Klein-Gordon equation on the unbounded domain. Then reduce the original problem (1.1) and (1.2) to an initial boundary value problem on a bounded computational domain, which can be solved by the finite difference method. By this numerical method, we observe the soliton solutions of different kinds of nonlinear Klein-Gordon equations.

The organization of this paper is as following: in Section 2, we give a brief overview of the operator splitting method, and then discuss the split local absorbing boundary for the NKLGE, where the ABCs of the subproblem is given in detail. A finite difference scheme is given by the coupling procedure in Section 3. Some numerical examples are provided to demonstrate the effectiveness of the proposed scheme, especially some interesting soliton solutions of the NLKGE are observed in Section 4.

2. The split local absorbing boundary method

Operator splitting method [26,34] is a powerful method for the numerical simulation of complex physical time-dependent models, where the simultaneous effect of several different subprocess has to be considered. Mathematical models of such phenomena are usually described by time-dependent partial differential equations, which include several spatial differential operators. Each of them is corresponding to a subprocess of the physical phenomenon. Generally speaking, every subprocess is simpler than the whole spatial differential operator.

The essential idea of the operator splitting method is to decompose the considered problem into several subproblems which are easy to be handled, and then solve them successively in a small time step τ, in which the solution of one subproblem is employed as the initial condition for the next subproblem.

The operator splitting method has been widely used in many application problems, for instance, the advection–diffusion-reaction problems in air pollution modelling [27] Maxwell's equations [28], the model of Bose–Einstein condensates [29,30] and the nonlinear Schrödinger equation [31,32].

The basic idea of split local absorbing boundary (SLAB) method is using the operator splitting method on the boundaries to construct boundary conditions. We decompose the nonlinear Klein-Gordon problem into linear and nonlinear subproblems on the artificial boundaries, which are easy to be handled, and then solve them alternatively in a small time step τ.

For Eq. (1.1), we introduce an auxiliary function $v = u_t$, and denote the vector function $U = (u, v)^{\mathrm{T}}$. Then Eq. (1.1) can be converted into a differential equation system:

$$U_t = \begin{pmatrix} u \\ v \end{pmatrix}_t = \begin{pmatrix} v \\ u_{xx} - f(u) \end{pmatrix}. \tag{2.1}$$

We introduce a splitting control parameter $\alpha \in (0,1)$, the previous system (2.1) can be written in a splitting form.

$$U_t = \begin{pmatrix} u \\ v \end{pmatrix}_t = \begin{pmatrix} \alpha^2 v \\ u_{xx} \end{pmatrix} + \begin{pmatrix} (1-\alpha^2)v \\ -f(u) \end{pmatrix} \equiv L_1 U + L_2(U). \tag{2.2}$$

From time $t = t^n$ to time $t = t^{n+1}$, where $t^{n+1} = t^n + \tau$, $t^0 = 0$, firstly we split the system (2.1) into a linear subproblem and a nonlinear subproblem.

$$U_t^1 = L_1 U^1 \quad U^1(t_n, x) = U(t_n, x) \quad t \in [t_n, t_{n+1}], \tag{2.3}$$

$$U_t^2 = L_2(U^2) \quad U^2(t_n, x) = U^1(t_{n+1}, x) \quad t \in [t_n, t_{n+1}]. \tag{2.4}$$

Then we solve the subproblems (2.3) and (2.4) step-by-step, in which the solution of one subproblem is employed as an initial condition for the alternative subproblem, and take $U(t_{n+1}, x) \approx U^2(t_{n+1}, x)$ as the approximate solution of the system (2.1). This may be realized by the solution operator that approximates combination of products of the exponential operators $e^{\tau L_1}$ and $e^{\tau L_2}$. By the Baker–Campbell–Hausdroff theorem, we have the first-order approximation using solution operator,

$$U^{n+1} \approx e^{\tau L_2} e^{\tau L_1} U^n. \tag{2.5}$$

So far, the simplest idea of the operator splitting method has been described. The error of the approximation (2.5) is the first-order $O(\tau)$ induced from the noncommutativity of the operators L_1 and L_2 [33]. In general, the second-order Strang splitting is more frequently adopted in applications, for which the solution operator is approximated by,

$$U^{n+1} \approx e^{\frac{\tau}{2} L_1} e^{\tau L_2} e^{\frac{\tau}{2} L_1} U^n. \tag{2.6}$$

In fact, the only difference between the Strang splitting method [34] and the first-order splitting method is that the first and last steps are half of the normal step τ. Thus a more accurate second-order method can be implemented by a very simple way.

Next, we use the operator splitting method to obtain the split local absorbing boundary (SLAB) conditions for the NKLGE. First of all, we introduce two artificial boundaries $\Sigma_l = \{(x,t) |\ x = x_l,\ 0 \leqslant t \leqslant T\}$ and $\Sigma_r = \{(x,t) |\ x = x_r,\ 0 \leqslant t \leqslant T\}$, where x_l, x_r are two constants, with $x_l < x_r$, which divide the unbounded domain $R^1 \times [0,T]$ into three parts,

$$D_l = \{(x,t) | -\infty \leqslant x \leqslant x_l, 0 \leqslant t \leqslant T\},$$
$$D_i = \{(x,t) | x_l \leqslant x \leqslant x_r, 0 \leqslant t \leqslant T\},$$
$$D_r = \{(x,t) | x_r \leqslant x \leqslant +\infty, 0 \leqslant t \leqslant T\}.$$

The finite sub-domain D_i is the bounded computational domain. Therefore, we must find some appropriate boundary conditions on Σ_l and Σ_r, respectively, to reduce the original initial value problem (1.1) and (1.2) into a initial boundary value problem on the domain D_i.

Some simple calculation shows that the equation of the linear subproblem (2.3) is equivalent to the following wave equations:

$$u_{tt} - \alpha^2 u_{xx} = 0. \tag{2.7}$$

In the problem (1.1) and (1.2), we assume the initial values $\phi_0(x), \phi_1(x)$ are constant in the exterior domain $D_l \cup D_r$. It means that no wave travels from the exterior domain into the interior domain D_i. So at the right artificial boundary Σ_r, we can obtain a absorbing artificial boundary condition (ABC):

$$u_t + \alpha u_x = 0,\ \forall (x,t) \in \Sigma_r. \tag{2.8}$$

Similarly, at the artificial boundary Σ_l, we can obtain a absorbing artificial boundary condition (ABC):

$$u_t - \alpha u_x = 0 \quad \forall (x,t) \in \Sigma_l. \tag{2.9}$$

The artificial boundary conditions (2.8) and (2.9) are linear transport equations, which can be discretized by the up-wind scheme or the beam-worming scheme, thus we have first- or second-order of accuracy, respectively. Similarly, the equation of the nonlinear subproblem (2.4) is equivalent to the following equation:

$$u_{tt} + (1-\alpha^2) f(u) = 0 \quad x_l \leqslant x \leqslant x_r \quad t^n \leqslant x \leqslant t^{n+1}. \tag{2.10}$$

The nonlinear Eq. (2.10) is an ordinary differential equation, which can be solved by the Runge–Kutta method or the Matlab ode-solver(ode15). Seeing that the restriction of (2.10) on the boundary Σ_l (or Σ_r) is an initial value problem, no extra boundary condition is required.

3. The derivation of the difference scheme

In this section, we consider the coupling procedure for solving the nonlinear Klein-Gordon equation on the bounded computational domain $D_i = [x_l, x_r] \times [0,T]$. We divide the domain D_i by a set of lines parallel to the x- and t-axis to form a grid, and

write $h = (x_l - x_r)/I$ and $\tau = T/N$ for the line spacings, where I and N are two positive integers. The crossing points Ω_h^τ are called the grid points,

$$\Omega_h^\tau = \{(x_i, t_n) | x_i = x_l + ih,\ i = 0, 1, \ldots, I,\ t_n = n\tau, n = 0, 1, \ldots, T/\tau\}.$$

Suppose $\mathbf{U} = \{u_i^n | 0 \leqslant i \leqslant I, n \geqslant 0\}$ is a grid function on Ω_h^τ. To get the numerical solution on the domain D_i, we use the central difference scheme to approximate Eq. (1.1):

$$\frac{u_i^{n+1} - 2u_i^n + u_i^{n-1}}{\tau^2} - \frac{u_{i+1}^n - 2u_i^n + u_{i-1}^n}{h^2} + f(u_i^n) = 0, \tag{3.1}$$

for $i = 1, \ldots, I-1$, where u_i^n represents the approximation of wave function $u(x,t)$ on the grid point (x_i, t^n) with $t^n = n\tau$, $x_i = ih$, $x_0 = x_l$, $x_I = x_r$.

For each computational step, the equation system (3.1) contains $I+1$ unknowns, however it only has $I-1$ equations. So the scheme (3.1) is incomplete, thus two unknown values u_0^n and u_I^n must be provided through boundary conditions. According to the discussion in Section 2, we split Eq. (1.1) into two subproblems (2.7) and (2.10) on the grid points (x_0, t^n) and (x_I, t^n) in the vicinity of the boundaries, and then solve them separately, in which the solution of one subproblem is employed as an initial condition for the next subproblem by imposing two intermediate variables $U_i^* = (u_i^*, v_i^*)^{\mathrm{T}}, i = 0, I$. For Eq. (2.10), we use the exponential operator form,

$$U_i^* \approx \mathrm{e}^{\tau L_2} U_i^n, \quad i = 0, I. \tag{3.2}$$

The second intermediate step is a linear problem, which can generate two extra equalities by discretizing the ABCs (2.8) and (2.9) with the up-wind scheme or the beam-worming scheme. Here, we take the up-wind scheme for an example,

$$\frac{u_I^{n+1} - u_I^*}{\tau} + \alpha \frac{u_I^* - u_{I-1}^n}{h} = 0, \tag{3.3}$$

$$\frac{u_0^{n+1} - u_0^*}{\tau} - \alpha \frac{u_1^n - u_0^*}{h} = 0. \tag{3.4}$$

At the $(n+1)$th time level, suppose $\{u_i^k | k \leqslant n, 0 \leqslant i \leqslant I\}$ are given. Firstly, we solve Eqs. (3.2)–(3.4) to get the boundary term $u_i^{n+1}, i = 0, I$ and assume $v_i^{n+1} = v_i^*$ then solve Eq. (3.1) to get $\{u_i^{n+1} | 1 \leqslant i \leqslant I-1\}$. Hence, we can get all the solution $\mathbf{U} = \{u_i^{n+1} | 0 \leqslant i \leqslant I, n \geqslant 0\}$ step-by-step. Compare with the global ABC as mentioned above, our split local absorbing boundary (SLAB) method has great advantage for long time computation. In order to improve the accuracy of the local time-splitting procedure, a second-order Strang splitting [34] and the beam-worming scheme can be used, where we use two intermediate variables $U_i^* = (u_i^*, v_i^*)^{\mathrm{T}}, i = 0, I$ and $U_i^{**} = (u_i^{**}, v_i^{**})^{\mathrm{T}}, i = 0, I$. Here, U_i^* is obtained from U_i^n through the half time step ordinary differential equation,

$$U_i^* \approx \mathrm{e}^{\frac{\tau}{2} L_2} U_i^n, \quad i = 0, I. \tag{3.5}$$

Suppose that $v_i^{**} = v_i^*, i = 0, I$ and $u_i^{**}, i = 0, I$ are deduced from $u_i^*, i = 0, I$ by the beam-worming scheme:

$$\frac{u_I^{**} - u_I^*}{\tau} = -\frac{\alpha(3u_I^* - 4u_{I-1}^n + u_{I-2}^n)}{2h} + \frac{\alpha^2(u_I^* - 2u_{I-1}^n + u_{I-2}^n)}{2h^2}, \tag{3.6}$$

$$\frac{u_0^{**} - u_0^*}{\tau} = \frac{\alpha(3u_0^* - 4u_1^n + u_2^n)}{2h} + \frac{\alpha^2(u_0^* - 2u_1^n + u_2^n)}{2h^2}. \tag{3.7}$$

Finally, U_i^{n+1} can be obtained from U_i^{**} through another half time step ordinary differential equation,

$$U_i^{n+1} \approx \mathrm{e}^{\frac{\tau}{2} L_2} U_i^{**}, \quad i = 0, I. \tag{3.8}$$

Thus a more accurate scheme can be obtained by coupling Eqs. (3.5)–(3.8) and the equation system (3.1).

4. Numerical tests

To test the performance and accuracy of the given split local absorbing boundary method, four different kinds of application examples for the NLKGE are provided in this section, where the second-order Strang splitting and the beam-worming scheme are used.

4.1. The sine-Gordon (sG) equation

The sine-Gordon (sG) equation is a very important nonlinear Klein-Gordon equation [19–21], which has the potential function $G(u) = 1 - \cos(u)$ and takes the following form:

$$\frac{\partial^2 u}{\partial t^2} - \frac{\partial^2 u}{\partial x^2} + \sin u = 0.$$

The sine-Gordon (sG) equation has some travelling soliton solutions, also called the kink solution and anti-kink solution.

$$u = 4\arctan\exp\left(\pm\frac{x-ct}{\sqrt{1-c^2}}\right),$$

where $c \in (0,1)$ is the moving velocity, the sign "+" corresponds to the case of kink solution, and "−" corresponds to the case of anti-kink solution. When $t = 0$, these solutions tend to some constants exponentially fast as x tends to infinity. For example, $u_{\text{kink}} \to 2\pi$ as $x \to +\infty$, and $u_{\text{kink}} \to 0$ as $x \to -\infty$.

First of all we consider the kink solution. Let $c = 0.8$, $x_l = -8$, $x_r = 8$ and take $\varphi_0(x) = u_{\text{kink}}(x,0)$ and $\varphi_1(x) = \frac{\partial}{\partial t}u_{\text{kink}}(x,0)$ as the initial data. From Fig. 1, we can see that the wave travels through the right artificial boundary, without causing dramatic reflection.

Next, we study the interaction of solitons, also called the Breather solution of the sine-Gordon equation. The sine-Gordon equation admits the kink–anti-kink solution,

$$u_{\text{kink-anti-kink}} = 4\arctan\left(\frac{c\sinh(\sqrt{c^2-1}t)}{\sqrt{c^2-1}\cosh(cx)}\right)$$

and the kink–kink solution,

$$u_{\text{kink-kink}} = 4\arctan\left(\frac{\sqrt{c^2-1}\sinh(cx)}{c\cosh(\sqrt{c^2-1}t)}\right).$$

The solitons in the kink–anti-kink solution(or the kink–kink solution) move with the same speed $\sqrt{c^2-1}/c$ but in different direction. Let $c = 2$, $x_l = -8$, $x_r = 8$ and take $\varphi_0(x) = u_{\text{kink-anti-kink}}(x,0)$, $\varphi_1(x) = \frac{\partial}{\partial t}u_{\text{kink-anti-kink}}(x,0)$ and $\varphi_0(x) = u_{\text{kink-kink}}(x,0)$, $\varphi_1(x) = \frac{\partial}{\partial t}u_{\text{kink-kink}}(x,0)$, respectively, as the initial data. Fig. 2 shows that the given scheme not only captures the interaction of solitons, but also let the solitons travel out the computational domain without causing dramatic reflection. Finally, we design an oscillation wave problem to test the performance of the given boundary conditions. In this case, $x_l = -8$, $x_r = 8$, the initial conditions are oscillation wave:

$$\varphi_0(x) = \sin(10x)\exp\left(-\frac{x^2}{4}\right), \quad \varphi_1(x) = 0.$$

Fig. 3 shows that the initial oscillation wave splits into two smaller waves and spreads along the characteristic lines. When they travel out the computational domain, the reflection waves are negligible.

4.2. The ϕ^4 equation

We also test the scheme for the travelling soliton wave of the ϕ^4 equation [20,21], which has the potential function $G(u) = -\frac{1}{2}m^2u^2 + \frac{1}{4}\gamma u^4$ and takes the following form:

$$\frac{\partial^2 u}{\partial t^2} - \frac{\partial^2 u}{\partial x^2} + \gamma u^3 - mu = 0,$$

where the m and γ are two parameters. The ϕ^4 equation has travelling soliton wave solutions, also called the kink and anti-kink solutions:

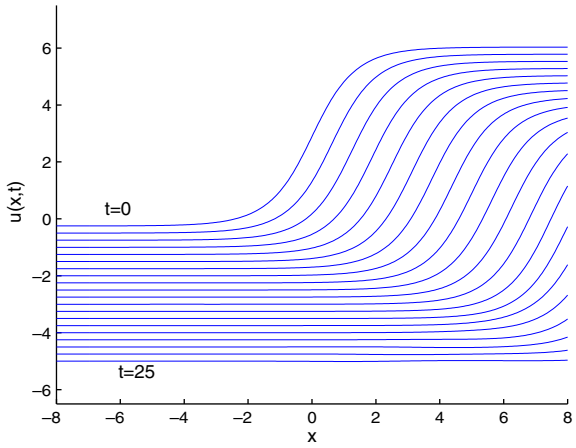

Fig. 1. Kink of the sine-Gordon equation, $h = 0.05$, $\tau = h/2$.

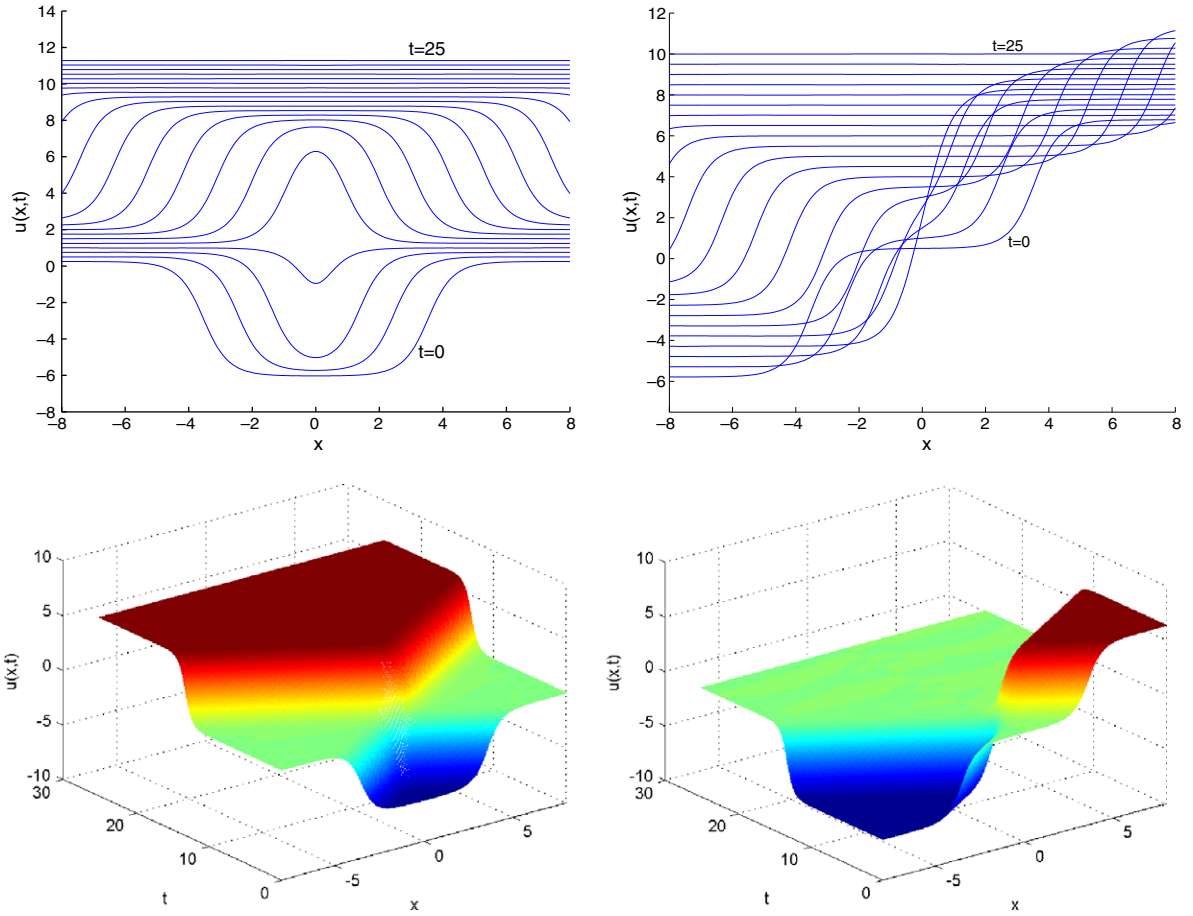

Fig. 2. Breather solution of the sine-Gordon equation, left are kink–anti-kink solutions and right are kink–kink solutions. $h = 0.05$, $\tau = h/2$.

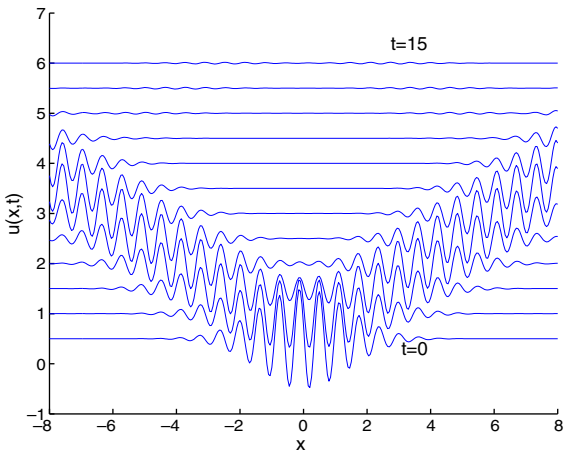

Fig. 3. Propagation of the oscillation wave of the sine-Gordon equation. $h = 0.05$, $\tau = h/2$.

$$u(x,t) = \frac{m}{\sqrt{\gamma}} \tanh\left(\pm \frac{m(x-ct)}{\sqrt{2(1-c^2)}}\right),$$

for $(x,t) \in R \times R^+$, with the velocity restricted by $c^2 < 1$. If we choose the sign "+" ("−"), the travelling soliton wave $u(x,t)$ is a kink(anti-kink) solution, i.e. it consists of a single transition region between the asymptotic values $u_{\text{kink}} = \pm 1 (u_{\textit{anti-kink}} = \mp 1)$

as $x - ct$ varies between $\pm\infty$. Again this solution is on the whole real line, and it quickly approaches its asymptotic values away from the transition region.

Similar to the construction of the soliton solution in Section 4.1, let $x_l = -8$, $x_r = 8$ and take $\varphi_0(x) = u_{\text{kink}}(x, 0)$ and $\varphi_1(x) = \frac{\partial}{\partial t} u_{\text{kink}}(x, 0)$ as the initial data. The numerical solutions of $u(x,t)$ is shown in Fig. 4, with $\gamma = \frac{1}{\pi^2}$, $m = 1$, $c = 0.8$ together with the step sizes $h = 0.05$ and $\tau = \frac{h}{2}$. We can see that the right artificial boundary is nearly transparent for the solitary wave propagation, since the wave travel out the computational domain without causing dramatic reflection.

4.3. The double sine-Gordon (DSG) equation

The double sine-Gordon (DSG) equation has attracted many researchers attention, because it models a variety of systems in condensed matter, quantum optics, and particle physics. Condensed matter applications include the spin dynamics of superfluid He^3, magnetic chains, commensurate-incommensurate phase transitions, surface structural reconstructions, and domain walls. In quantum field theory and quantum optics DSG equation applications include quark confinement and self-induced transparency, respectively, see [22,23]. The double sine-Gordon (DSG) equation has the potential,

$$G(u) = -\frac{4}{1+4|\eta|}\left(\eta\cos u - \cos\frac{u}{2}\right),$$

where the parameter η may be assigned any arbitrary real value. In this paper we will consider the range $\eta > 0$, so we introduce parameter R related with η by $\eta = \frac{1}{4}\sinh^2 R$. From the potential function $G(u)$, we get the following DSG equation:

$$\frac{\partial^2 u}{\partial t^2} - \frac{\partial^2 u}{\partial x^2} + \frac{2}{1+4|\eta|}\left(2\eta\sin u - \sin\frac{u}{2}\right) = 0. \tag{4.1}$$

Eq. (4.1) has a static solution in the form of a 4π kink (anti-kink):

$$u(x,t) = 4\pi m \pm 4\arctan\frac{\sinh\left(\frac{x-ct}{\sqrt{1-c^2}}\right)}{\cosh R},$$

where the sign "+" corresponds to the case of kink, and "−" corresponds to the case of anti-kink, and m is an integer. $u(x,t)$ can be interpreted as a superposition of two sG solitons, separated by the distance $2R$.

In the numerical experiment, we set $c = 0.8$, $x_l = -12$, $x_r = 12$ and take $\varphi_0(x) = u_{\text{kink}}(x, 0)$ and $\varphi_1(x) = \frac{\partial}{\partial t} u_{\text{kink}}(x, 0)$ as the initial data. The numerical solutions of $u(x,t)$ is shown in Fig. 5, with $m = 0$, $R = 4$, together with the step sizes $h = 0.05$ and $\tau = \frac{h}{2}$. We can find that the profile of the initial wave consists two kinks. They travel through the right artificial boundary consecutively, without causing dramatic reflection, which shows that the boundary conditions are nearly transparent for the wave propagation.

4.4. The double sinh-Gordon (DSHG) equation

The double sinh-Gordon (DSHG) equation has been extensively studied in the classical thermodynamics. This model equation also has a double well potential $G(u) = (\zeta\cosh 2u - m)^2$, when the positive parameter m, ζ satisfy $m > \zeta$, thus there also exists the kink and anti-kink solutions. Even though it is nonintegrable, the DSHG is remarkably amenable to analysis, see[24,25]. From the potential function $G(u)$, we get the following DSHG equation:

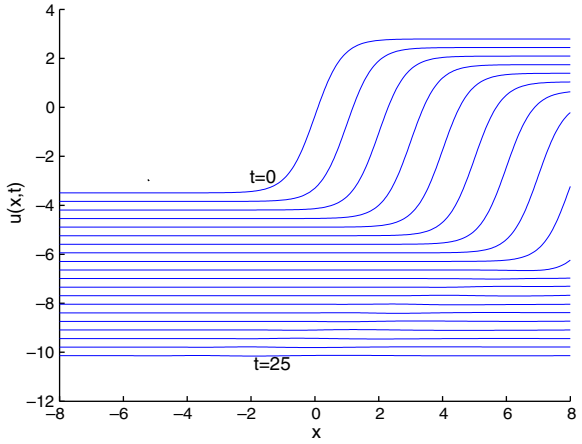

Fig. 4. Kink of the ϕ^4 equation, $h = 0.05$, $\tau = h/2$.

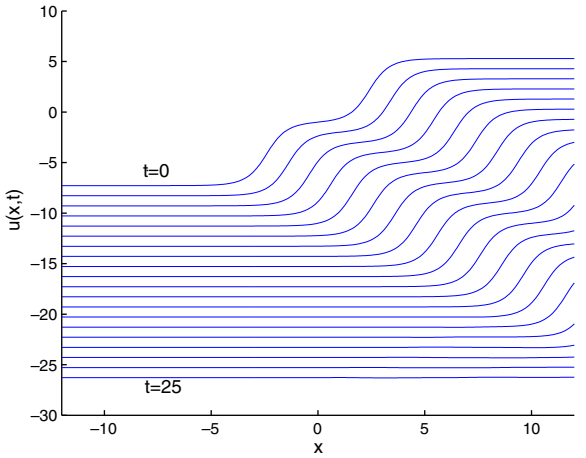

Fig. 5. Double kink of the DSG equation, $h = 0.05$, $\tau = h/2$.

$$\frac{\partial^2 u}{\partial t^2} - \frac{\partial^2 u}{\partial x^2} + 2\zeta(\zeta \sinh 4u - 2m \sinh 2u) = 0. \tag{4.2}$$

Eq. (4.2) possess a single kink solution and anti-kink solution as following:

$$u(x,t) = \pm \tanh^{-1}\left(\sqrt{\frac{m-\zeta}{m+\zeta}} \tanh \xi \frac{x - ct}{\sqrt{1-c^2}}\right), \quad \xi = \sqrt{2(m^2 - \zeta^2)},\ m > \zeta.$$

The sign "+" corresponds to the case of kink solution, and the sign "−" corresponds to the case of anti-kink solution. Eq. (4.2) can be linearized around $u = 0$ leading to higher energy phonons. For phonons around $u = 0$, the above Eq. (4.2) can be approximated by a ϕ^4 equation, which shows the connection between the ϕ^4 equation and the DSHG equation.

$$\frac{\partial^2 u}{\partial t^2} - \frac{\partial^2 u}{\partial x^2} + (8\xi^2 - 8m\xi)u + \frac{16}{3}(4\xi^2 - m\xi)u^3 = 0.$$

In the numerical experiment, we set $c = 0.5$, $x_l = -8$, $x_r = 8$ and take $\varphi_0(x) = u_{\text{kink}}(x, 0)$ and $\varphi_1(x) = \frac{\partial}{\partial t} u_{\text{kink}}(x, 0)$ as the initial data. The numerical solutions of $u(x,t)$ is shown in Fig. 6, with $m = 2$, $\xi = 1$, together with the step sizes $h = 0.05$ and $\tau = \frac{h}{2}$. We can see that the kink solution travels through the right artificial boundary without causing dramatic reflection, which shows that the boundary conditions are also effective for this nonintegrable equation.

4.5. Accuracy of the SLAB method

In this section, we consider the numerical accuracy of the SLAB method for the tested problems in Sections 4.1–4.4 with exact solutions. Numerical experiments show that for these four kinds of nonlinear Klein-Gordon equation, the SLAB method

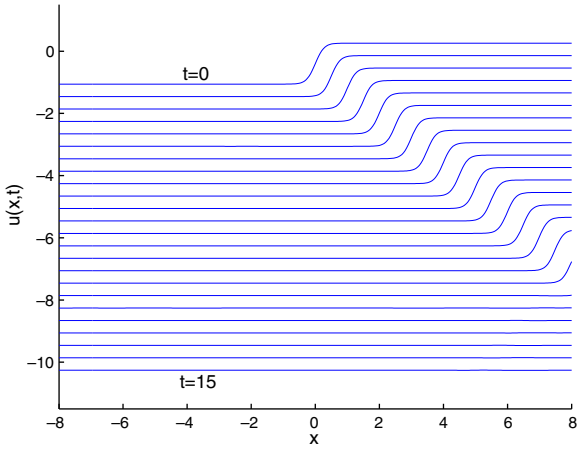

Fig. 6. Kink of the DSHG equation, $h = 0.05$, $\tau = h/2$.

has the same accuracy. To avoid tautology, we only give the numerical results about the sG equation and the ϕ^4 equation here.

In all the computation, we let $h = 2\tau$. To evaluate the accuracy of numerical solution, we define the L_2 norm of the error function as

$$E(t) = \|u_{\text{num}}(\cdot, t) - u_{\text{exa}}(\cdot, t)\|_{L_2}. \tag{4.3}$$

Table 1 lists the errors for different mesh sizes and the convergence rates. Fig. 7 gives the linear least square fitting of different errors and mesh sizes in logarithm coordinates. It can be seen that our numerical scheme is second-order convergence, just as we anticipate.

Fig. 8 gives the result about how the SLAB method depends on the cut points x_l and x_r. The top-left part is the evolution of the sG equation with $h = 0.05, \tau = \frac{h}{2}, x_l = -15, x_r = 15, T = 22.5$. The initial value on the top-right part shows that the wave-

Table 1
Computation of $E(12)$ and the convergence order, $h = 2\tau$

Mesh size	L_2 norm of the error (sG equation)	L_2 norm of the error (ϕ^4 equation)
$h = \frac{1}{10}$	1.713E−2 ...	2.212E−2 ...
$h = \frac{1}{20}$	4.262E−3 4.019	5.532E−3 4.011
$h = \frac{1}{40}$	1.066E−3 3.996	1.383E−3 3.999
$h = \frac{1}{80}$	2.739E−4 3.893	3.459E−4 3.998
$h = \frac{1}{160}$	9.345E−5 2.930	8.666E−5 3.991

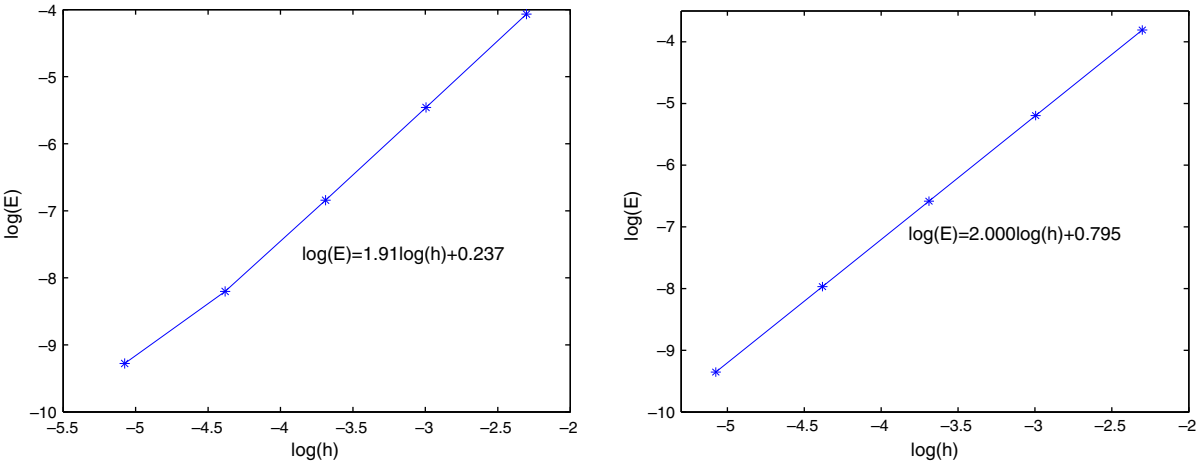

Fig. 7. Linear least square fitting of different errors and mesh sizes, left is sG equation, right is ϕ^4 equation. $h = \frac{1}{10}, \frac{1}{20}, \frac{1}{40}, \frac{1}{80}, \frac{1}{160}, \tau = \frac{h}{2}$.

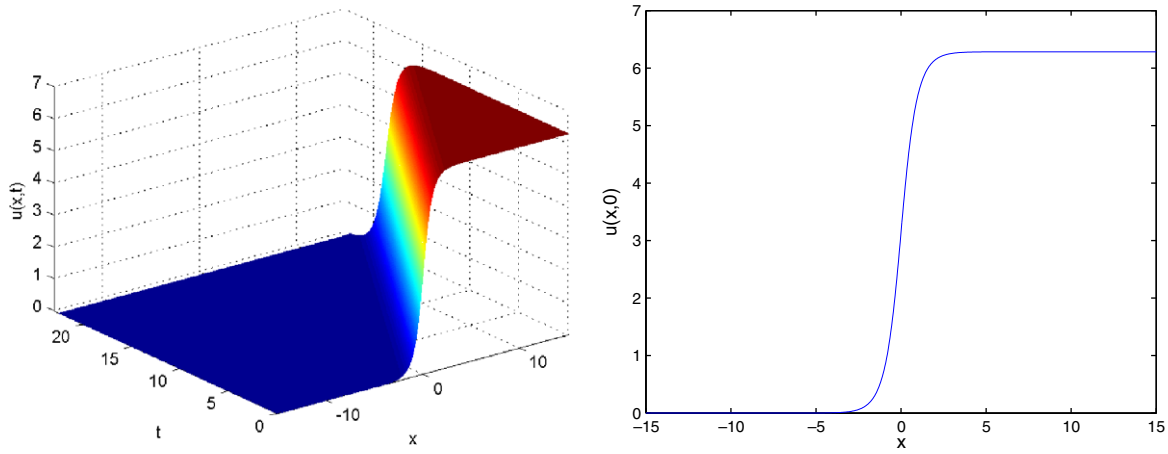

Fig. 8. The waveform of the sG equation, $h = 0.05$, $\tau = h/2$, $T = 22.5$.

form is constant outside the interval $[-5,5]$. Let $L = |x_l| = |x_r|$ denotes the distance from the location of the artificial boundary to the center of the computational domain. During the computation process, we fix the terminal time as $T = 22.5$. Initially, we set $L = 1$ and every time we increase L by 1 to compute the numerical error. Here, the error function is defined by

$$E(L) = \max_{0\leqslant t\leqslant T,-L\leqslant x\leqslant L} |u_{\text{num}}(x,t) - u_{\text{exa}}(x,t)|.$$

Fig. 9 shows that when the length L is bigger than 5, the SLAB method will have a very high numerical accuracy.

The choice of the splitting control parameter α is quite important in the SLAB method, however how to get the α in an analytic way is still open. Through numerical experiments, we find that if we choose the splitting control parameter $0.8 < \alpha < 0.9$, the given method is nearly transparent for the wave propagation. Hence, in all of the numerical experiments in this paper, we set $\alpha = 0.85$. Fig. 10 shows the numerical error for different velocity of the sG equation. Here, the error function is the same as (4.3), and the wave velocities are $c = 0.8$ and $c = 0.4$, respectively.

The numerical schemes (3.1)–(3.4) are the standard splitting method, hence we call them SLAB1 for simplicity. Similarly, the Strong splitting methods (3.1) and (3.5)–(3.8) are called SLAB2. We compare the performance of these two methods for sG equation and ϕ^4 equation. Fig. 11 shows that the SLAB2 method is second-order convergence, but when the mesh size is fine enough, the SLAB1 method can not get the second-order convergence. For the nonlinear Klein-Gordon equation on the unbounded domain, Szeftel [35] adopted the paradifferential calculus approach to construct a family of absorbing boundary conditions for the semilinear wave equation. Let PDC1 and PDC2 denote the first- and second-order absorbing boundary conditions given by Szeftel. In fact, the PDC1 absorbing boundary condition is just the Neumman boundary condition. We compare the performance of the PDC1, PDC2 and SLAB2 method for the sG equation and ϕ^4 equation.

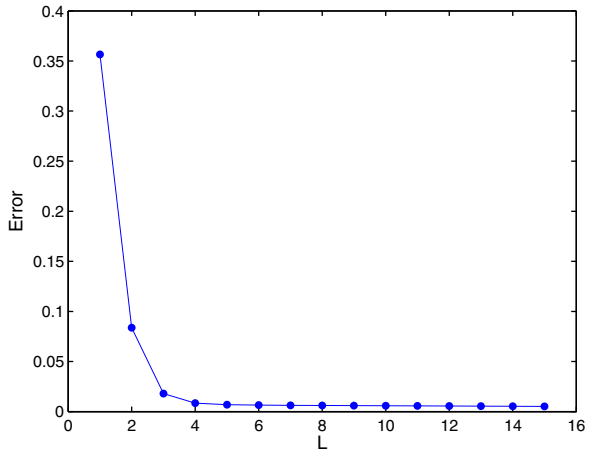

Fig. 9. The errors of different length L for the sG equation, $h = 0.05$, $\tau = h/2$, $T = 22.5$.

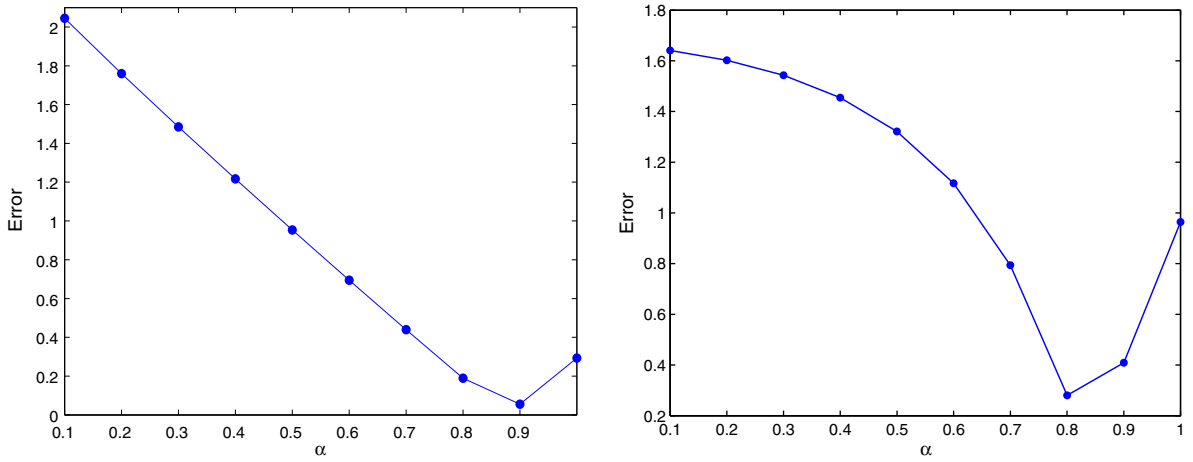

Fig. 10. The errors of different splitting control parameter α for the sG equation, $h = 0.05$, $\tau = h/2$, $T = 12$. Left is $c = 0.8$, right is $c = 0.4$.

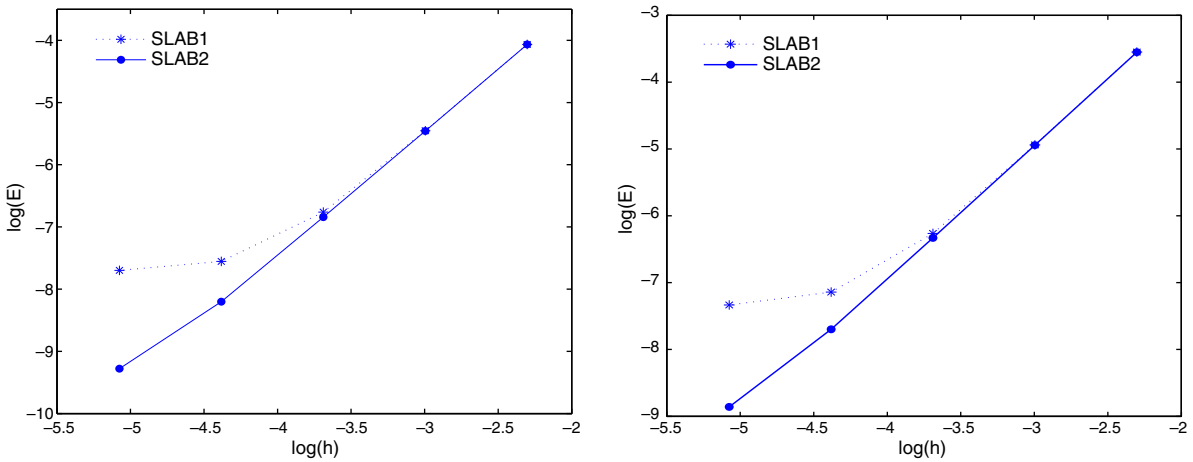

Fig. 11. Comparison between the standard and Strong splitting methods, $h = 0.05$, $\tau = h/2$, $T = 12$. Left is sG equation, right is ϕ^4 equation.

Figs. 12 and 13 show that for a large-range of wave velocity c, the SLAB2 method is nearly transparent for the wave propagation, which means the SLAB2 method is robust to wave velocity c. When $c = 0.8$ the PDC2 method is more accurate than the SLAB2 method. However, when the wave velocity is small, the PDC2 method will bring strong reflection on the artificial

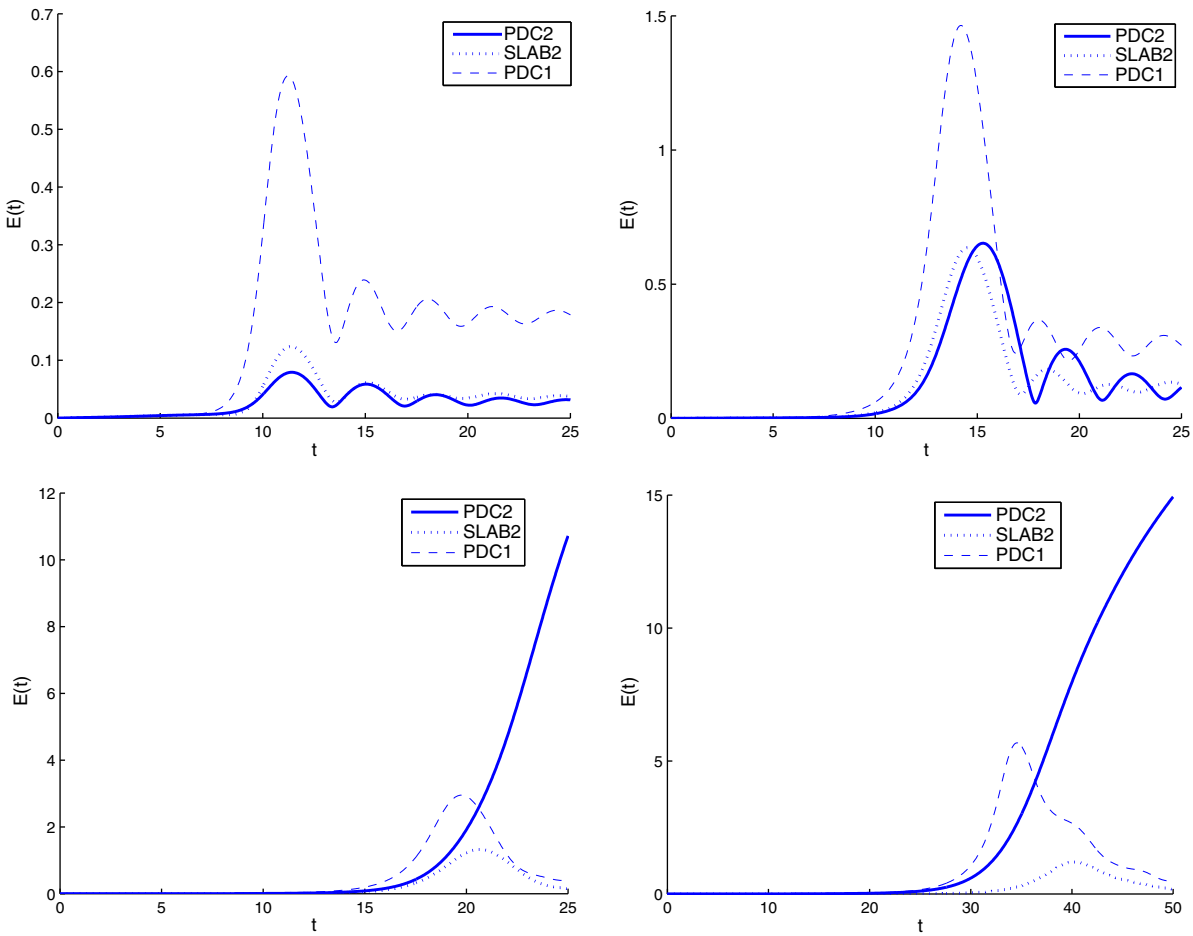

Fig. 12. Comparison of different absorbing boundary conditions for the sG equation, $h = 0.05$, $\tau = h/2$. From top-left to bottom-right $c = 0.8, 0.6, 0.4, 0.2$, respectively.

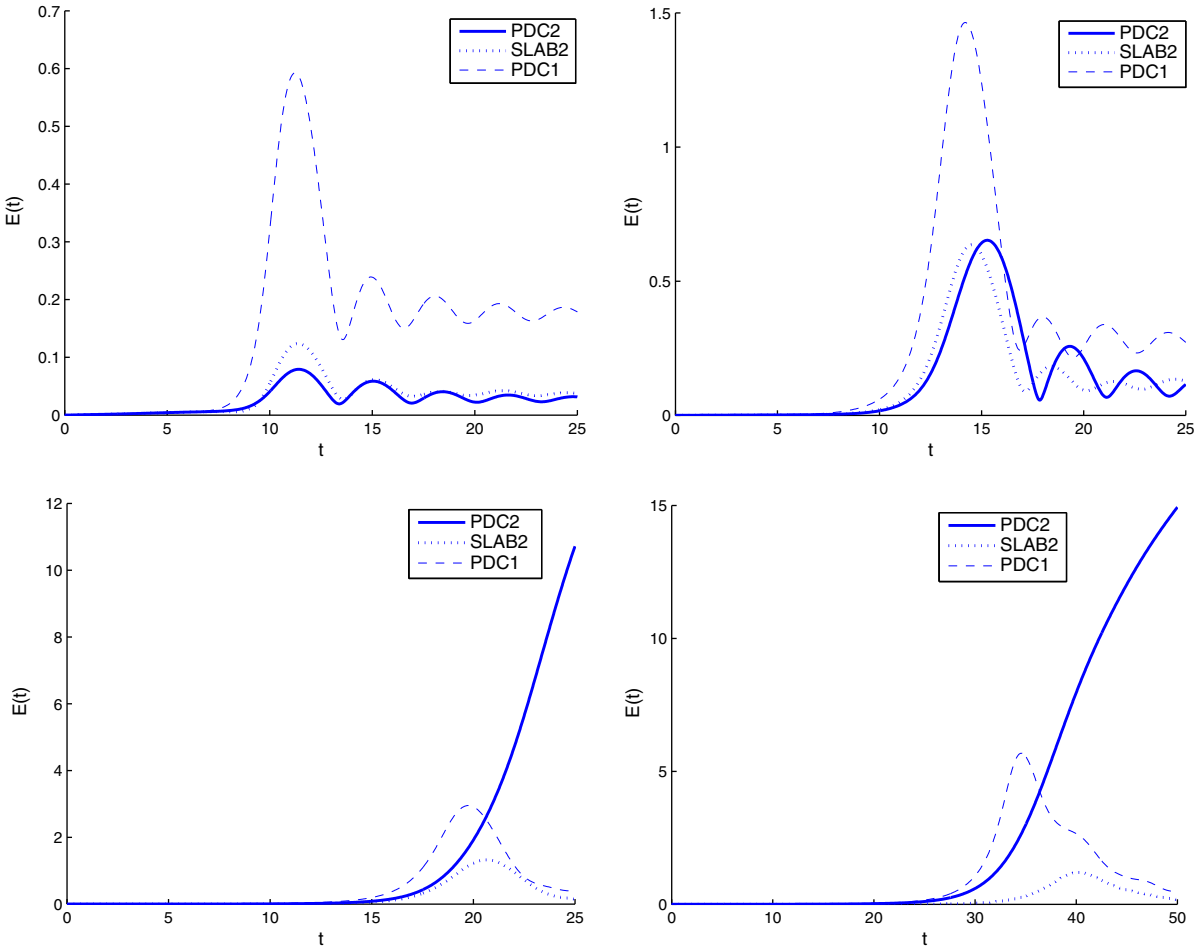

Fig. 13. Comparison of different absorbing boundary conditions for the ϕ^4 equation, $h = 0.05$, $\tau = h/2$. From top-left to bottom-right $c = 0.8$, 0.6, 0.4, and 0.2, respectively.

boundaries. We can also see that for the nonlinear Klein-Gordon equation, the Neumman (PDC1) boundary conditions will cause dramatic reflection.

5. Conclusion

The numerical solution of the one-dimensional nonlinear Klein-Gordon equation on an unbounded domain is studied in this paper. Split local absorbing boundary (SLAB) conditions are obtained by the operator splitting method, then the original initial value problem is reduced to an initial boundary value problem on a bounded computational domain. Numerical examples indicate that the given method is fast and nearly transparent for the wave propagation, but the stability and error analysis of the method is still open. This method also has the potential of generalizing to multi-dimensional nonlinear Klein-Gordon equation on the unbounded domain, which we will be our further work.

Acknowledgment

This work is supported by the National Natural Science Foundation of China (Grant No. 10471073).

References

[1] R.K. Dodd, J.C. Eilbeck, J.D. Gibbon, H.C. Morris, Solitons in Nonlinear Wave Equations, Academic Press, New York, 1982.
[2] P.J. Drazin, R.S. Johnson, Soliton: An Introduction, Cambridge University Press, Cambridge, UK, 1989.
[3] S. Li, L. Vu-Quoc, Finite difference calculus invariant structure of a class of algorithms for the nonlinear Klien-Gorodn equation, SIAM J. Numer. Anal. 32 (6) (1995) 1839–1875.
[4] S. Jiminez, Derivation of the discrete conservation laws of a family of finite difference schemes, Appl. Math. Comput. 64 (1994) 13–45.

[5] S. Jiminez, L. Vazquez, Analysis of four numerical schemes for a nonlinear Klein-Gordon equation, Appl. Math. Comput. 35 (1990) 61–94.
[6] B.Y. Guo, X. Li, L. Vazquez, A Legendre spectral method for solving the nonlinear Klein-Gordon equation, J. Comput. Appl. Math. 15 (1) (1996) 19–36.
[7] B.Y. Guo, P.J. Pascual, M.J. Rodriguez, L. Vazquez, Numerical solution of the sine-Gordon equation, Appl. Math. Comput. 18 (1986) 1–14.
[8] B. Engquist, A. Majda, Absorbing boundary conditions for the numerical simulation of waves, Math. Comput. 31 (1986) 629–651.
[9] D. Givoli, High-order local non-reflecting boundary conditions: a review, Wave Motion 39 (2004) 319–326.
[10] T. Hagstrom, Radiation boundary conditions for the numerical simulation of waves, Acta Numer. 8 (1999) 47–106.
[11] H. Han, The Artificial Boundary Method–Numerical Solutions of Partial Differential Equations on Unbounded Domains, Frontier and Prospects of Contemporary Applied Mathematics, Higher Education Press, World Scientific, 2005.
[12] B. Alpert, L. Greengard, T. Hagstrom, Rapid evaluation of nonreflecting boundary kernel for time-domain wave propagation, Acta Numer. 8 (1999) 47–106.
[13] M.J. Grote, J.B. Keller, Exact nonreflecting boundary conditions for the time dependent wave equation, SIAM J. Appl. Math. 55 (2) (1995) 280–297.
[14] H. Han, C. Zheng, Exact nonreflecting boundary conditions for an acoustic problem in three dimensions, J. Comput. Math. 21 (1) (2003) 15–24.
[15] Z. Teng, Exact boundary condition for the time-dependent wave equation based on boundary integral, J. Comput. Phys. 190 (2003) 398–418.
[16] H. Han, X. Wu, Z. Xu, Artificial boundary method for Burger's equation using nonlinear boundary conditions, J. Comput. Math. 24 (2006) 295–304.
[17] Z. Xu, H. Han, X. Wu, Numerical method for the deterministic Kardar–Parisi–Zhang equation in unbounded domains, Commun. Comput. Phys. 1 (2006) 479–493.
[18] C. Zheng, Exact nonreflecting boundary conditions for one-dimensional cubic nonlinear Schrödinger equations, J. Comput. Phys. 215 (2006) 552–565.
[19] C. Zheng, Numerical solution to the sine-Gordon equation defined on the whole real axis, SIAM J. Sci. Comp. 29 (6) (2007) 2494–2506.
[20] Z. Fei, L. Vazquez, Two energy conserving numerical schemes for the sine-Gordon equation, Appl. Math. Comput. 45 (1994) 17–30.
[21] D.B. Duncan, Symplectic finite difference approximations fo the nonlinear Klein-Gordon equation, SIAM J. Numer. Anal. 34 (5) (1997) 1742–1760.
[22] V. Gani, A. Kudryavtsev, Kink–antikink interactions in the double sine-Gordon equation and the problem of resonance frequencies, Phys. Rev. E 60 (3) (1999) 3305–3309.
[23] S. Burdick, M. El-Batanouny, C.R. Willis, Internal dynamics of the double-sine-Gordon chain, Phys. Rev. B 34 (9) (1986) 6575–6579.
[24] S. habib, A. khare, A. Saxena, statistical mechanics of double sinh-Gordon kinks, Physica D 123 (1998) 341–356.
[25] S. habib, A. khare, A. Saxena, Exact thermodynamics of the double sinh-Gordon theory in $1 + 1$ dimensions, Phys. Rev. Lett. 79 (20) (1997) 3797–3801.
[26] S. Yu, S. Zhao, G.W. Wei, Local spectral time splitting method for first- and second-order partial differential equations, J. Comput. Phys. 206 (2005) 727–780.
[27] D. Lanser, J. Verwer, Analysis of operator splitting for advection–diffusion-reaction problems in air pollution modelling, J. Comput. Appl. Math. 111 (1-2) (1999) 201–216.
[28] L. Gao, B. Zhang, D. Liang, The splitting finite-difference time-domain methods for Maxwell's equations in two dimensions, J. Comput. Appl. Math. 205 (1) (2007) 207–230.
[29] W. Bao, S. Jin, P. Markowich, On the time-splitting spectral approximations for the Schrödinger equation in the semiclassical regime, J. Comput. Phys. 175 (2002) 487–524.
[30] W. Bao, S. Jin, P. Markowich, Numerical study of time-splitting spectral discretizations of nonlinear Schrödinger equation in the semi-classical regime, SIAM J. Sci. Comp. 25 (2003) 27–64.
[31] Z. Xu, H. Han, Absorbing boundary conditions for nonlinear Schrödinger equations, Phys. Rev. E 74 (2006) 037704.
[32] Z. Xu, H. Han, X. Wu, Adaptive absorbing boundary conditions for Schrödinger-type equations: application to nonlinear and multi-dimensional problems, J. Comput. Phys. 225 (2) (2007) 1577–1589.
[33] L.A. Khan, P.L.F. Liu, Numerical analyses of operator-splitting algorithms for the two-dimensional advection–diffusion equation, Comput. Meth. Appl. Mech. Eng. 152 (1998) 337–359.
[34] G. Strang, On the construction and comparison of difference schemes, SIAM J. Numer. Anal. 5 (1968) 506–517.
[35] J. Szeftel, A nonlinear approach to absorbing boundary conditions for the semilinear wave equation, Math. Comput. 75 (2006) 565–594.